

REPORT DOCUMENTATION PAGE		READ INSTRUCTIONS BEFORE COMPLETING FORM
1. REPORT NUMBER	2. GOVT ACCESSION NO.	3. RECIPIENT'S CATALOG NUMBER
4. TITLE (and Subtitle) "Correlation and Collective Modes in Narrow Band Materials"		5. TYPE OF REPORT & PERIOD COVERED Final -- Oct. 1, 1981 to Sept. 30, 1985
		6. PERFORMING ORG. REPORT NUMBER
7. AUTHOR(s) Martin W. Riharsky		8. CONTRACT OR GRANT NUMBER(s) AFOSR--80--0023
9. PERFORMING ORGANIZATION NAME AND ADDRESS Georgia Institute of Technology School of Physics Atlanta, Georgia 30332		10. PROGRAM ELEMENT, PROJECT, TASK AREA & WORK UNIT NUMBERS
11. CONTROLLING OFFICE NAME AND ADDRESS Air Force Office of Scientific Research Bolling AFB, Building 410 Washington, D. C. 20332		12. REPORT DATE May 15, 1986
		13. NUMBER OF PAGES
14. MONITORING AGENCY NAME & ADDRESS (if different from Controlling Office)		15. SECURITY CLASS. (of this report)
		15a. DECLASSIFICATION/DOWNGRADING SCHEDULE
16. DISTRIBUTION STATEMENT (of this Report) Approved for public release; Distribution unlimited.		
17. DISTRIBUTION STATEMENT (of the abstract entered in Block 20, if different from Report)		
18. SUPPLEMENTARY NOTES		
19. KEY WORDS (Continue on reverse side if necessary and identify by block number) Transition metals, copper, correlation, excitons, dielectric response, interband excitation, optical spectra, energy loss spectra, superconductivity.		
20. ABSTRACT (Continue on reverse side if necessary and identify by block number) Correlation, collective modes, and localized bonding states have been studied for systems with quite localized valence or conduction bands or for metal systems with adsorbates. One aspect of this research has been concerned with localized electron-hole states and how they contribute with other excitations to the dynamical response of the system. Important problems studied have been the effects of exciton or exciton-like states on superconducting properties, electron energy loss spectra, and optical spectra. In this part of the		

(continued)

research CuCl was studied using a tight-binding model. The results show that strong effects due to localized excitations of d-band electrons make off-diagonal matrix elements of the inverse dielectric matrix important and also show that the exchange interaction greatly affects the excitation spectrum, producing exciton resonances in the band gap. These effects in turn make strong contributions to the loss spectra and optical spectra. Models have also been set up to relate the dynamical response, including local field effects, to the superconducting transition temperature and gap function. Calculations have been done that confirm the analysis of high resolution electron energy loss spectra for water adsorbed on copper surfaces. The nature of the localized bond between the water molecule and copper surface atoms and the orientation and vibrational modes of the water molecule were established and are supported by experiment.

Table of Contents

	page
I. Research Objectives.	1
II. Studies of Narrow Band Materials and Localized Bonding	3
III. Local Field and Exchange Effects in the Dielectric Response.	5
A. Tight Binding Calculations	5
B. Model of Superconductivity Including Local Field and Exchange Effects	7
IV. Tight Binding Calculations of the Dielectric Response for CuCl	10
V. Water Monomers on Cu (100): Localized Bonding	21
VI. References	29

I. Research Objectives

The overall objective of this work was to study correlation and collective modes for systems with quite localized valence or conduction bands. For these systems one must consider the effects of localized excitations and collective modes to understand large scale correlated states such as superconductivity or the interaction of the system with optical or electronic probes. In certain cases, such as for narrow-band insulators, one must consider these effects to understand even ground state properties. In particular this research has been concerned with localized electron-hole states and excitonic modes and how they contribute with other excitations to the dynamical response of the system.

The effect of strongly localized excitations on the superconducting properties of a material can be significant. We have been most concerned with the effect on the superconducting mechanism itself. For systems such as oxidized Cu or CuCl, there are some experimental indications that the usual phonon-coupling mechanism is augmented or even dominated by an exciton-coupling mechanism. We have developed some models to describe the excitation structure in terms of excitons alone and with these have studied local field effects on the dynamical response.

The effects of localized excitations on the response to optical or electronic probes is known to be significant. Our exciton models have already successfully explained the optical absorption due to intrinsic excitons in several materials. Our objective here has been to provide a detailed description of the effects of local field corrections and umklapp scattering terms on the dielectric response of these materials. The calculations described in this report show that the local field corrections are important in general for tightly-bound systems and in particular for impurity-doped CuCl under pressure. Also,

the calculations reveal a rich exciton resonance structure that is quite sensitive to the strength of the electron exchange interaction, and that provides possibly new and important details about the nature of the excitonic states in narrow band systems.

Our models have led to a clearer picture of the superconducting state in narrow band materials. Also we have obtained a better understanding of the electronic excitation structure of these systems and of the structure of the optical absorption and electron energy loss spectra. In addition we have developed methods for describing the effect of correlations between metal and adsorbate valence electrons on the bonding and vibrational excitations of metal-adsorbate systems. We will discuss these calculations further below.

II. Studies of Narrow Band Materials and Localized Bonding

We have developed several theoretical methods and models for dealing with the electronic structure and properties of narrow band materials and of localized bonding. Among these are:

1. Tight-binding models - These are models which describe the d- and s-valence band electronic structure of materials. They can be used to give the density of states of transition metals, alloys and compounds.

2. Surface and grain boundary segregation models - Using the tight-binding density of states and minimizing the system free energy, one can obtain the surface and grain boundary composition. We have extended this model to the surface segregation of ternary alloys and are extending it to include d-band effects in grain boundary segregation. We have also developed a model for the diffusion of a non-uniform implant profile in the presence of a surface. The model shows that considerable nonequilibrium implant surface segregation can occur under certain conditions even if there is no equilibrium surface segregation.

3. Excitonic Superconductivity Models - We have used the tight-binding model to develop a model for excitonic effects on the attractive effective electron-electron coupling which includes local field effects and the effects of valence and conduction band structure. We have also developed a model for the superconducting transition temperature and gap equation which includes local field and excitonic effects.

4. Cluster calculation methods - We have extensive experience with ab-initio Hartree-Fock and linear-combination-of-atomic orbitals $X\alpha$ (LCAOX α) molecular cluster methods. These methods give a detailed description of local electronic structure and they are self-consistent so that they describe the rearrangement of the electrons even for changes in complicated geometries. In particular the methods are useful for defects in the bulk or at surfaces or

boundaries, for studying certain localized catalytic and adsorption processes, and for systems of complicated local geometries which are likely to have localized electronic states. We have extended the methods to long range systems by applying embedding models which include the dominant effects of the environment on the cluster. Our recent calculations are for H₂O adsorbed on Cu surfaces where we explore the correlation of Cu d and s electrons with O p and s electrons to produce surface-adsorbate bonds. Our calculations give the first detailed agreement between theory and experiment for H₂O monomers on a Cu surface and provide a complete description of the bonding mechanism for this important system. Papers and presentations during the grant period in the general area of properties of transition metals or narrow band materials are:

"Exciton Coupling and the Effective Electron Interaction in Narrow Band Materials," A. P. S. March Meeting, Los Angeles (1983).

"Local Field Effects on Exciton Coupling in CuCl and CdS Under Pressure," High Pressure in Science and Technology (Elsevier, New York, 1984).

"Local Field Effects Due to Excitons and the Superconducting Coupling Constant," A. P. S. March Meeting, Detroit (1984).

"The Diffusion of Implanted Ions near Surfaces and Grain Boundaries," A. P. S. March Meeting, Detroit (1984).

"Electronic Structure Calculations of Water on a Copper Surface," 44th Physical Electronics Conference (June, 1984).

"Molecular Orbital SCF Cluster Model of H₂O Adsorption on Copper," A. P. S. March Meeting, Baltimore (1985).

"Effects of Local Fields on the Superconducting Mechanism," A. P. S. March Meeting, Baltimore (1985).

"A Molecular Orbital SCF Cluster Model of H₂O Adsorption on Copper," Phys. Rev. B. 32, 1430 (1985).

III. Local Field and Exchange Effects in the Dielectric Response

A. Tight Binding Calculations

Our tight binding model is based on a model developed by Prakash and Joshi¹ and extended by Hanke to the lattice dynamics of Pd and Ni.² One assumes that the band structure of the system is adequately described by a non-interacting band model. Then one connects the high-symmetry points in the band structure according to compatibility and which atomic level they represent by symmetry (for example Γ_{12} connects with L_3 in FCC structures because both states represent $d_{m=2}$). The bands are then described as parabolas with an effective mass assigned to give them the optimal shape. The Bloch states in the tight-binding formulation are just

$$\psi_{\nu}^{\vec{k}}(\vec{r}) = \frac{1}{N^{1/2}} \sum_{\ell} e^{i\vec{k} \cdot \vec{R}_{\ell}} u_{\nu}(\vec{r} - \vec{R}_{\ell}),$$

where u_{ν} is the appropriate atomic wave function. Although these approximations are fairly extreme, the model dielectric screening, when used in calculations of the phonon dispersion for Pd and Ni, gives good results.²

The simplest band model for the metallic systems of interest here is an s-d band model. We can augment this model by assuming the d bands are hybridized with, for example O or Cl p states in the case of the oxide or chloride of Cu. In the s-d band model, the dielectric matrix is

$$\underline{\underline{\epsilon}} = \underline{\underline{1}} - \underline{\underline{\epsilon}}_{ss} - \underline{\underline{\epsilon}}_{sd} - \underline{\underline{\epsilon}}_{ds} - \underline{\underline{\epsilon}}_{dd}. \quad (1)$$

When d-d intraband terms contribute, our calculations³ indicate that $\underline{\underline{\epsilon}}_{dd}$ dominates in Eq. (1). Hanke also found this to be the case for Pd and Ni.²

However, for calculations of the superconductivity properties where the exciton positions and strengths are important, one cannot neglect the s-d interband terms since they contribute to the exciton structure. To simplify the present

where

$$\underline{\underline{S}} = \underline{\underline{N}}^0 \left[\underline{\underline{1}} - \left(\underline{\underline{V}} - \frac{1}{2} \underline{\underline{V}}^x \right) \underline{\underline{N}}^0 \right]^{-1},$$

and the non-interacting polarizability $\underline{\underline{N}}^0$ is given in Eq. (2.10) of Ref. 4 with all expansion coefficients C set equal to one.

It is apparent from Eqs. (1-3) that we have a frequency- and momentum-dependent formulation of the dielectric matrix including exchange which is in terms of few important parameters. The Coulomb and exchange interactions in Eq. (2) are comprised of only three and four elements, respectively, for the case of d-d interband and intraband transitions in CuCl. The magnitude of each element depends on the extent of the atomic-like wave function on Cu. The widths and frequency positions of structures in $\underline{\underline{N}}^0$ depend directly on the energy band widths and positions. The positions and dispersions of excitons and plasmons in $\underline{\underline{\epsilon}}^{-1}$ will then depend on combinations of these quantities. Thus by evaluating the dependence of the dielectric response and exciton and plasmon structures on these parameters and then tabulating the values of these parameters for many materials, we may know the trends in correlation and collective phenomena for a wide range of narrow band systems. We present some results from such an evaluation in Sec. IV.

B. Model of Superconductivity Including Local Field and Exchange Effects

The purpose of this section is to describe a model for a superconducting state in terms of Coulomb interactions alone. Thus the dielectric response of the surrounding medium must be included explicitly to obtain an attractive interaction between electrons. The dielectric response is frequency dependent and contains exchange interactions so that one may evaluate the strength of both the exciton and plasmon pairing mechanisms.

We have developed a method in terms of Bloch states which includes the effects of the dynamical dielectric response on the superconducting properties.⁵ The method follows the development of Takada,⁶ except that it is generalized to a Bloch basis set to take into account local field effects. Our expression for the critical temperature T_c is

$$T_c = 1.134 \epsilon_F \exp \left[\frac{1}{\beta_{no}} + \int_{-1}^{\infty} \frac{dx}{2|x|} \sum_{n_3} \frac{\Delta_{n_3}(x)}{\Delta_n(o)} \right]$$

$$K_{nn_3}(o,x)/\beta_{no} = \theta(1-|x|) \quad , \quad (4)$$

$$x \equiv \omega/\epsilon_F \quad ,$$

where

$$\beta_{no} \equiv \sum_{n_3} \frac{\Delta_{n_3}(o)}{\Delta_n(o)} K_{n_3 n_3}(o,o) \quad ;$$

n, n_3 refer to Bloch states; ϵ_F is the Fermi energy; and Δ_n is the gap function. The kernel K is a generalization of the usual homogeneous form (see Ref. 6) which contains the screened interaction

$$\underline{\underline{\epsilon}}^{-1}(\vec{p}, \vec{q}, \omega) \underline{\underline{V}}(\vec{p}, \vec{q})_s$$

where $\underline{\underline{V}}$ is the Coulomb interaction matrix in the Bloch basis. This form of $\underline{\underline{\epsilon}}^{-1}$ is just the one we considered in the last section using the tight-binding model.

In addition, we obtain an expression for $\phi_n(x) = \Delta_n(x)/\Delta_n(o)$:

$$\phi_n(x) = K_{n,n}(x,o)/K_{nn}(o,o) \quad (5)$$

$$= \int_{-1}^{\infty} \frac{dx'}{2|x'|} \sum_{n_3} \frac{\Delta_{n_3}(x')}{\Delta_n(o)} \left[K_{nn_3}(x,x') - \frac{K_{nn}(x,o)}{K_{nn}(o,o)} K_{nn_3}(o,x) \right]$$

We can treat Eq. (5) as a linear integral equation and solve for $\phi_n(x)$ and then find T_C using Eq. (4). Equations (4) and (5) are new results for inhomogeneous periodic systems which reduce to the previously found homogeneous equations.⁶

IV. Tight-Binding Calculations of the Dielectric Response for CuCl

Experimental measurements of anomalously large diamagnetism⁷⁻⁹ in CuCl samples under pressure from 5 to 15 kb and at temperatures up to 240° have stirred considerable interest in the possibility of high temperature superconductivity. Calculations of the valence and conduction bands¹⁰⁻¹² all indicate CuCl is a direct gap semiconductor with a zincblende structure and that it remains so under the pressures used in the experiments. However, Collins, et al.¹³ have proposed a mechanism for the anomalous diamagnetism based on the presence of impurity levels such as 0^{--} just below the conduction band edge. They suggest that under pressure the X point moves down and that the 0^{--} levels pressure-ionize to produce free carriers around the X point. The lowering of the X point under pressure to a position degenerate with the Γ point is supported by the calculations of Kunz and Weidman.¹⁰ Collins et al.¹³ then show that an exciton-mediated high temperature super-conducting state can exist assuming an appropriate exciton-electron interaction and density of free carriers. Nobody, however, has addressed the fundamental question of whether the exciton-mediated electron-electron interaction is attractive. This is the purpose of the present calculations.

The equilibrium valence band structure for CuCl¹¹ is divided into three non-overlapping regions as shown in Fig. 1. The lowest VB1 band is 90% Cl 3s character and is between 10 and 12 eV from the predominantly (75%) Cl 3p VB2 band. In our calculations we are only interested in the mostly Cu 3d VB3 band which is 3.5 eV above VB2. The VB3 band has a lower, nearly dispersionless subband and a higher subband 1.5 eV wide which contains 24% Cl 3p and 76% Cu 3d character at the zone center. The magnitude of these orbital hybridizations agrees well with experimentally-deduced values based on exciton spin-orbit splitting (25% Cl 3p)¹⁴ and other measurements. The lowest conduction band CB1 is mostly Cu 4s at the zone center but has d-p character at $X_3(3)$. The calculations show that the valence bands remain unchanged for moderate lattice contractions, but the conduction bands drop

at the BZ edge.¹⁰⁻¹² The insert in Fig. 1 shows the bands VB3 and CB1 in the calculation of Kunz and Weidman.¹⁰ Here a 1% lattice contraction, consistent with the pressure used by Chu et al.⁸ in their diamagnetism measurements, has rendered the points Γ_1 and X_3 nearly degenerate.

We have rendered the bands of Kunz and Weidman in the effective mass approximation so that the band energy is

$$E_{nk} = E_{on} + \frac{\hbar^2 k^2}{2m_n}$$

where m_n is the effective mass and E_{on} is the energy at the bottom of the band. For the VB3 bands we have used the Γ and X points to determine the effective masses (see Prakash and Joshi for details)¹ and have ignored the non-degeneracy at X in the two subbands. For the conduction bands we have connected $\Gamma_{15}(3)$ to $X_3(3)$ and $\Gamma_1(2)$ to $X_1(3)$ because these pairs are s-like and d-p like, respectively,¹⁵ and we must connect points allowing the same symmetry when we assume non-hybridized bands.¹ The curvatures of the bands near $X_3(3)$ and $X_1(3)$ suggest an avoided crossing of this type. The zone boundary at X is at .615 a.u. for CuCl; but because we are using a spherical approximation for the energy bands, it is appropriate to use the Wigner-Seitz sphere radius to define the Fermi momentum. This value is .605 a.u. All the band structure parameters are given in Table I.

Since the upper valence band and the lowest conduction band at the X point have Cl 3p character as well as Cu 3d character, we must take hybridization into account. We can do this by allowing the conduction bands to be a Cu 3d-Cl 3p anti-bonding state. This hybridization is allowed because both Γ_{15} and X_3 can have d-p character. We use a mixing of 75% Cu and 25% Cl for the bonding state and 25% Cu and 75% Cl for the anti-bonding state. Besides being consistent with the experiment, this result is in agreement with calculations at Γ_{15} .¹² For the

atomic Cu 3d levels we choose the wavefunction obtained by Wachters,¹⁶ and for the Cl 3p levels we use the wavefunctions of Veillard.

In the calculations of the dielectric response reported here, we have used the above model for CuCl under pressure. We have assumed a small concentration of free carriers resides at the conduction band X point (degenerate with the Γ point in this case), and we have neglected excitations from the valence bands to the s-like conduction bands around Γ . Since d-d transitions dominate the dielectric matrix²⁹ this is a good approximation for calculations where exciton structure is not important. Such is the case for the optical absorption away from the exciton peaks for this system, or for the dielectric response of the four-fold coordinated compounds of Zn or Cd, which do not have s-like lowest conduction bands. However, for calculations of superconducting properties, the dp-s transitions should be included because the exciton structure is important. Nevertheless, even for this case the following calculations give useful results.

We can study local field effects in our test system by looking at the matrix elements of $\underline{\epsilon}^{-1}(\vec{q}, \omega)$ defined in Sec. IIIA. If local field effects were important, off-diagonal matrix elements would be large. Therefore we compare in Fig. 2a the matrix elements $\underline{\epsilon}^{-1}_{V2C;V2C}$ and $\underline{\epsilon}^{-1}_{V2C,CC}$ where V2C signifies transitions from the top valence band to the conduction band and CC signifies intraband transitions from filled to empty conduction band states. The momentum chosen for these calculations is $.103q_f$, and the energy range, 0.05–0.20 a.u. (1.36 – 5.44 eV), is in the band gap of our test system. Thus, $\underline{\epsilon}^{-1}(\vec{q}, \omega)$ is real, and there is no absorption except at the exciton poles. Note that since we have ignored dp-s transitions, our system acts as if it had an indirect gap. If we included the lowest s conduction band, the band gap would only be .150 a.u. The results in Fig. 3a show that the off-diagonal element $\epsilon^{-1}_{V2C,CC}$ is indeed significant over the whole frequency range and that local field effects cannot be ignored. To determine its dependence on lattice vector, we plot $\epsilon^{-1}_{V2C,V2C}$ (at $\vec{R} = \vec{R}' = 0$) versus $\epsilon^{-1}_{V2C,V2C;1,1}$ at the first lattice vector ($\vec{R} = \vec{R}' = a/2(1,1,0)$) in Fig. 3b. Again we find $\epsilon^{-1}_{V2C,V2C;1,1}$

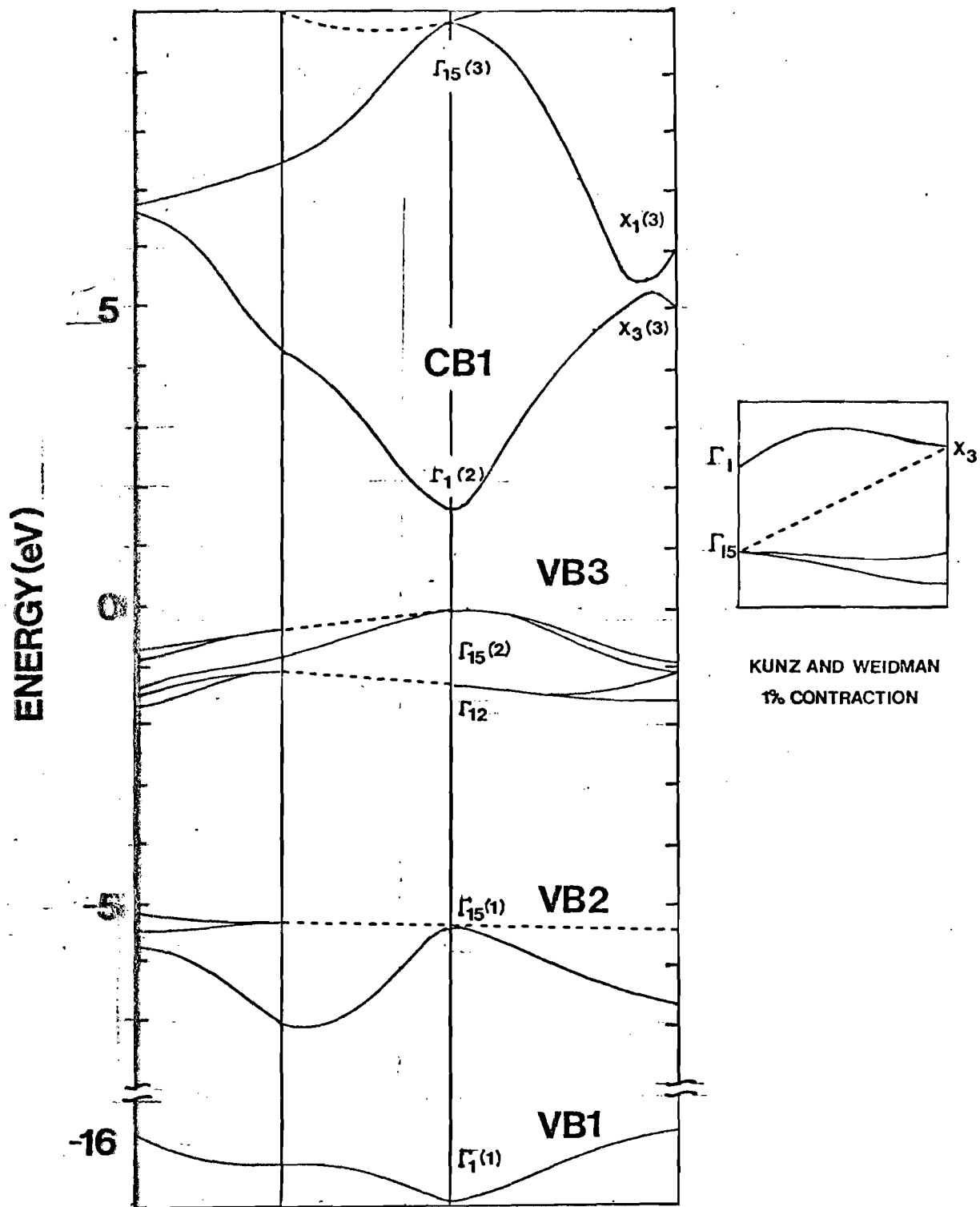


Fig. 1 EQUILIBRIUM ENERGY BANDS OF CuCl

TABLE I. Band structure parameters for CuCl under 1% contraction

lattice parameter crystal structure	10.215 a.u. zincblende	energy levels at high symmetry points (a.u.)
effective masses (in units of m_e):		Γ_{12} -.250
$m\{\Gamma_{12} - (X_1, X_2)\}$	20	$\Gamma_{15}(2)$ -.105
$m\{\Gamma_{15}(2) - (X_3, X_5)\}$	-2.21	$\Gamma_1(2)$.045
$m\{\Gamma_1(2) - X_1(3)\}$	1.28	$\Gamma_{15}(3)$.220
$m\{\Gamma_{15}(3) - X_3(3)\}$	-1.05	$X_1(2), X_2$ -.241
		$X_5(2), X_3(2)$ -.188
		$X_3(3)$.045
		$X_1(3)$.188

Band Gap: .150 a.u. (4.08 ev)

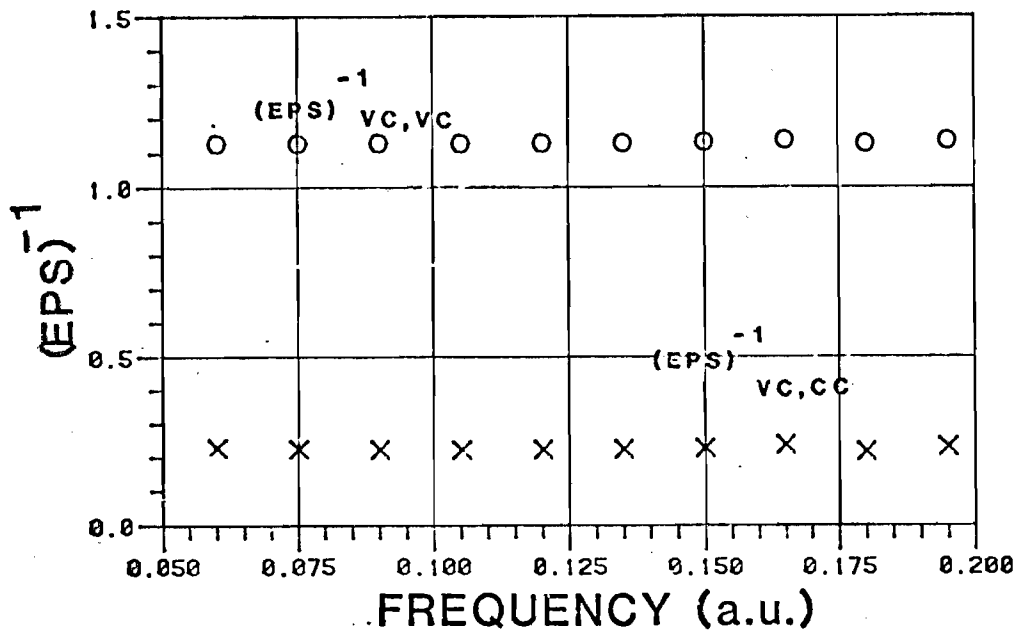


Fig. 2a Comparison of the matrix elements $\epsilon^{-1}_{V2C,V2C}$ and $\epsilon^{-1}_{V2C,CC}$ at $q = .103 q_f$.

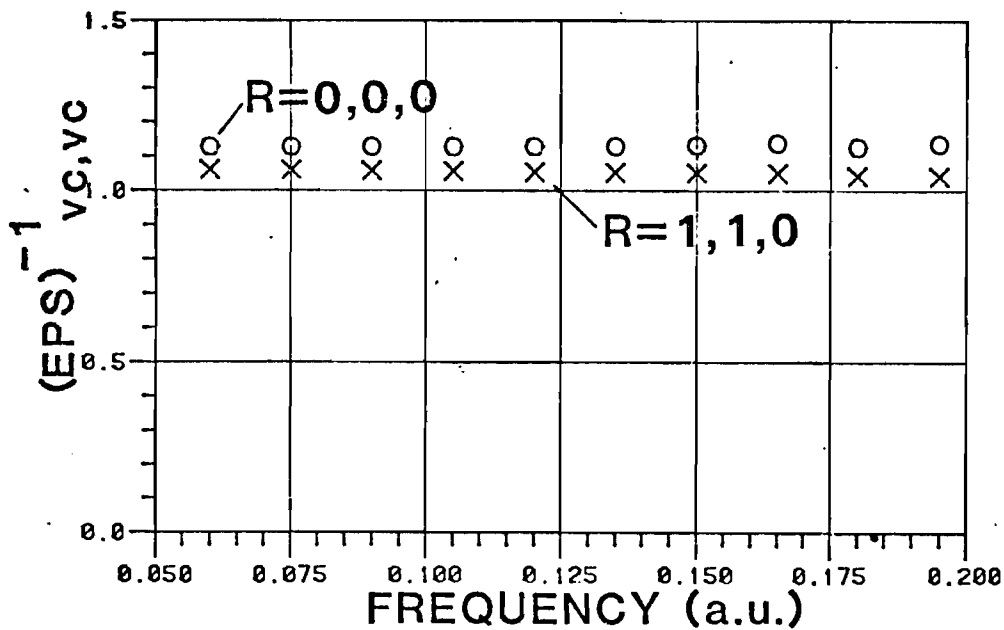


Fig. 2b Comparison of $\epsilon^{-1}_{V2C,V2C}$ at $\vec{R}=(0,0,0)$ and $\vec{R}=a/2(1,1,0)$ for $q = .103 q_f$.

to be significant so that we cannot neglect the dependence on lattice vector. In fact, we find it necessary to include through next nearest neighbor lattice vectors so that we have matrix elements for 19 vectors for the V2C,V2C transition. Our conclusions show that the recent model for the dielectric response of Fiorino and Del Sole,¹⁷ which only includes terms for $\vec{R} = \vec{R}' = 0$ is greatly oversimplified.

The exciton pole structure is interesting to study because it illuminates the dynamical structure of $\underline{\underline{\epsilon}}^{-1}(\vec{q}, \omega)$. True excitons exist only in the band gap, where there is no absorption. The true excitons are at the poles of $\underline{\underline{\epsilon}}^{-1}$ which are determined by the zeros of the factor

$$\left[\underline{\underline{1}} - (\underline{\underline{V}} - \frac{1}{2}\underline{\underline{V}}^X) N^0 \right]$$

in Eq. (3). We find the zeros by searching for the frequency at which the determinant Det of this factor is zero. In Fig. 3a we show the results for Real (Det) at $q = .103q_f$. As one can see, Real (Det) crosses zero only once in the band gap for this q , and thus there is only one exciton. The insert in Fig. 3a shows the region of the crossing in detail and can be used to determine the strength of the exciton since

$$\text{Det} \approx f (\omega - \omega_{\text{ex}})$$

near the pole ω_{ex} , where f is the strength. We find the exciton to be quite strong so that it should produce a higher transition temperature in our model. We can see the effect on the screened interaction by looking at the matrix element $(\underline{\underline{\epsilon}}^{-1}\underline{\underline{V}})_{\text{CC,CC}}$ in Fig. 3b. As we noted in Sec. IIIB, this matrix element determines the dynamics of the kernel K in the superconducting gap function. The matrix element goes dramatically negative, as it should, for frequencies greater than ω_{ex} indicating the attractive interaction which results in superconductivity.

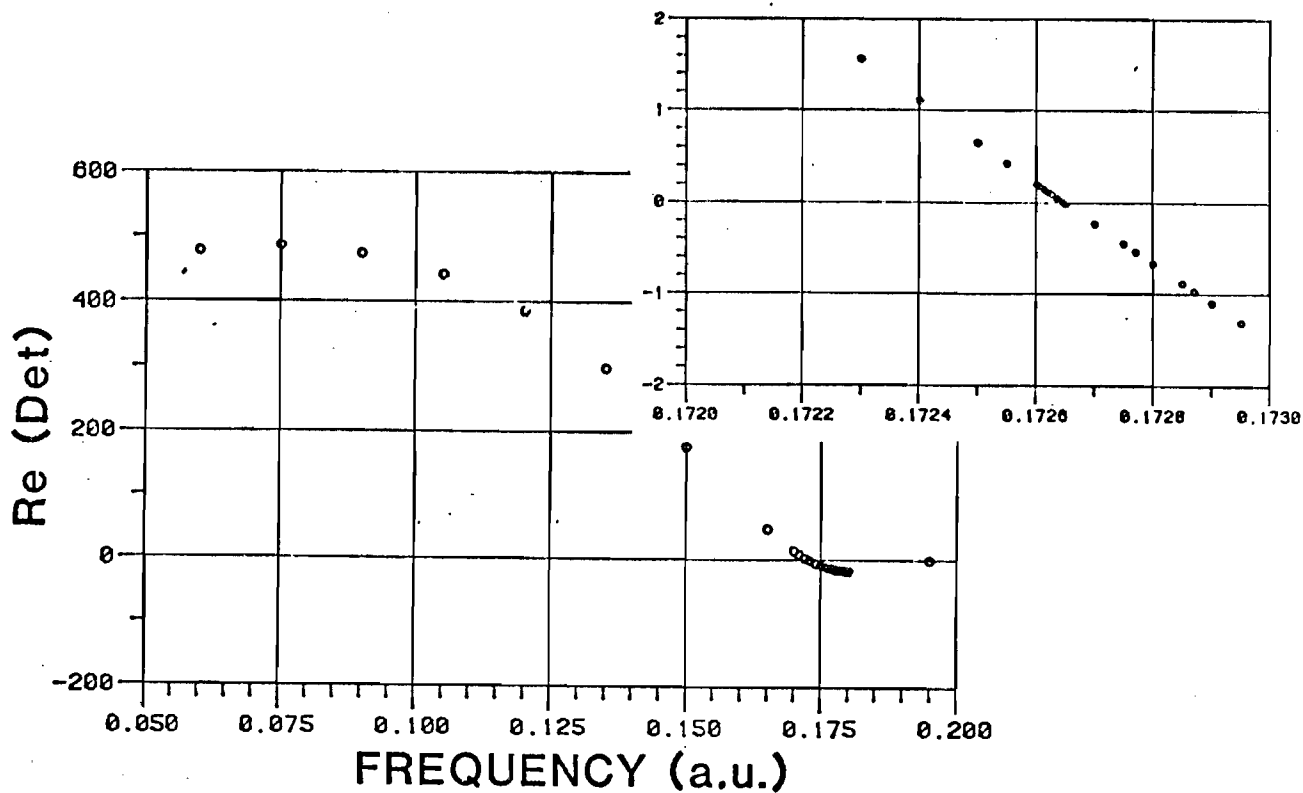


Fig. 3a Real part of the determinant of $[\underline{1 - (\underline{V} - \frac{1}{2} \underline{V}^x) \underline{N}}^0]$ at $q = .103 q_f$.

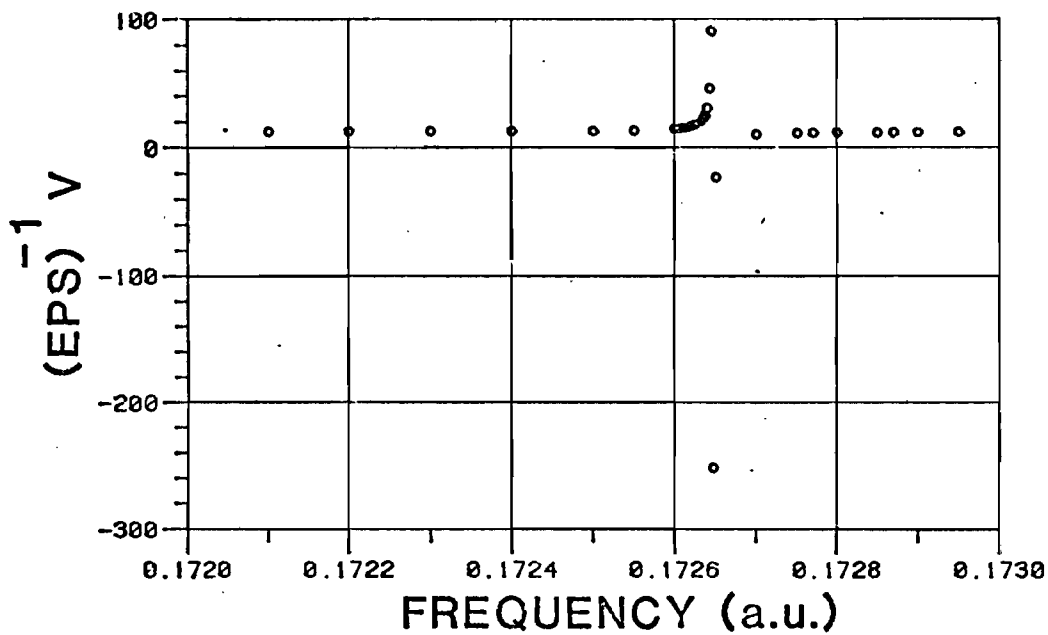


Fig. 3b Real part of $(\underline{\epsilon}^{-1} \underline{V})_{CC,CC}$ at $q = .103 q_f$.

The frequency positions of excitons and exciton-like structures in the dielectric response are determined by the magnitude of the elements in \underline{V}^x . As these matrix elements diminish in magnitude, the exciton moves to higher frequency and eventually disappears. We can see this effect in Fig. 4 where we plot Real (Det) for $\underline{V}^x = 0$. The exciton pole has disappeared from the band gap. These results show that one can vary the magnitudes of the elements in \underline{V}^x to match the experimental exciton energies and thus gain important information about the exchange interaction.

We may also study the dependence of the excitons on momentum q . We compare Real (Det) for $q = .103q_f$ with that for $q = .2q_f$ in Fig. 5. For excitations from our valence bands to the dp -like conduction bands, the gap diminishes for larger q values. Thus we see a crossing of zero at lower frequency for $q = .2q_f$, but we also see several other crossings as well. It may seem surprising that so many exciton poles appear in a system with only two valence bands and one conduction band and only a few distinct exchange matrix elements. But the maximum number of poles allowed is determined by the dimensionality of the $\underline{\epsilon}^{-1}$ matrix, and thus excitons can arise from elements with non-zero \vec{R} . For example, in our system there would be 19 possible exciton poles for each interband excitation. This is a fascinating aspect of the exciton pole structure which has not been studied before.

The effects of exciton-like transitions on the interband absorption part of the dielectric response also came out of our calculations, but we do not present those results here. We are now adding the more complicated dp to s excitation terms to our dielectric response formalism, and when that is done we will have a complete formulation for CuCl .

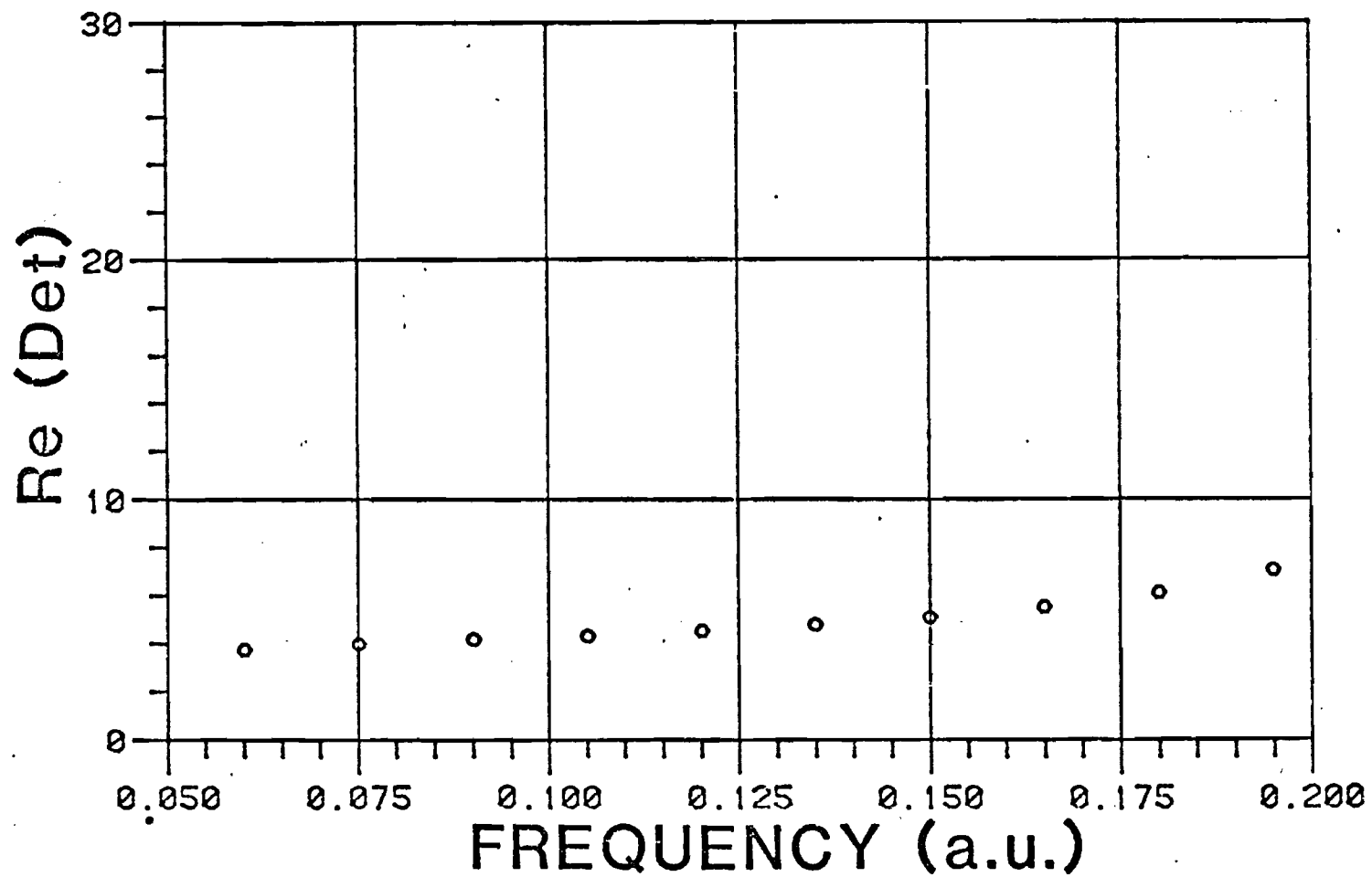


Fig. 4 Real part of determinant defined in Fig. 4a for $\underline{V}^x=0.0$ at $q = .103 q_f$.

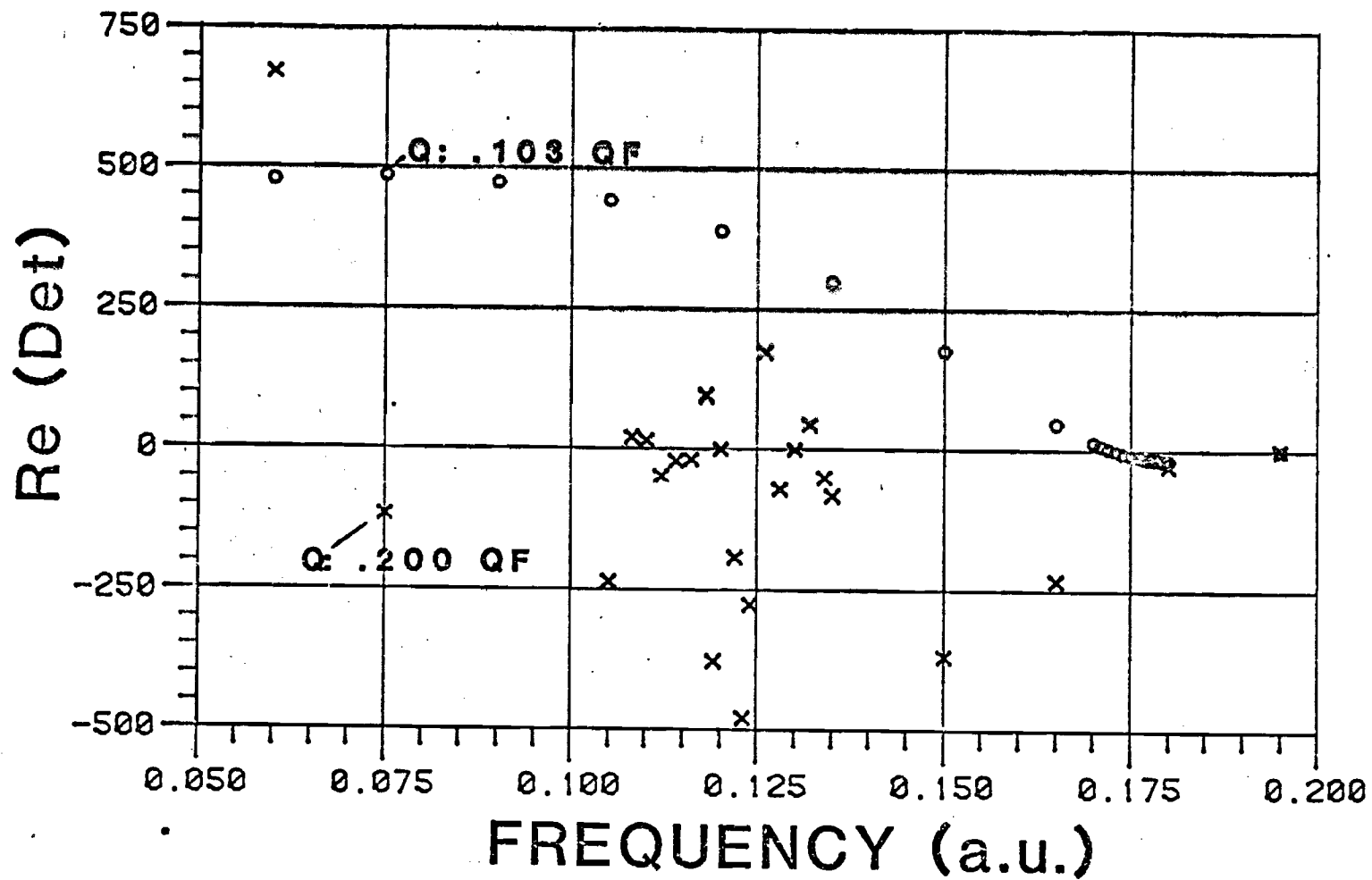


Fig. 5 Real part of determinant defined in Fig. 4a at $q = .103 q_f$ and $q = .200 q_f$.

V. Water Monomers on Cu (100): Localized Bonding

We have recently used another approach to describe the local electronic configurations and the correlation which comes about via bonding in adsorbate-metal surface systems. We have used linear combination of atomic orbitals X_α ¹⁸ (LCAO X_α) cluster calculations to study H_2O monomers on a Cu surface. Recently experimentalists have isolated these monomers on a metal surface for the first time and studied them with high resolution EELS.¹⁹ Understanding the nature of the bonding for this system is important due to the physical and chemical processes involving H_2O that are of fundamental and technological interest such as corrosion, certain catalytic reactions and electrochemical processes in aqueous solution. We have elucidated the bonding mechanism for this system,²⁰ and our results can be generalized to other H_2O -metal surface systems.

The self-consistent field X_α method has successfully described the details of bonding in many chemisorbed systems. With the LCAO version that we use, one obtains analytic electron wavefunctions that can easily be used to calculate properties. In the X_α method, the non-local exchange interaction is replaced by a local approximation, and the electron density-dependent Hamiltonian equation is solved iteratively until a self-consistent electron density is found (i.e., the electron density derived from the Hamiltonian solution is the same as the one used to construct the Hamiltonian). The self-consistency allows the atomic potentials to respond properly to changes in geometry, or to the effects of surface or adsorbed molecules. Because of the local exchange approximation, the X_α method can solve for larger clusters much more efficiently than non-local methods (e.g., Hartree-Fock or generalized valence bond).

The impetus for our investigations was provided by the electron-energy-loss spectroscopy (EELS) experiments of Andersson, Nyberg, and Tengstal¹⁹ of water adsorption on Cu(100) at low temperatures ($T \sim 10$ K) and low coverages in which evidence for H₂O monomer molecular adsorption has been found. Assignment of vibrational modes and analysis of spectral intensities allowed them to conclude that the water molecule is bonded to the metal via the oxygen with the molecular H₂O axis tilted approximately 60° away from the surface normal.

Our calculations simulated the local interactions between an H₂O molecule and a Cu surface with two clusters: a small cluster containing H₂O and one Cu atom (H₂O-Cu) and a larger cluster with H₂O and 5 Cu atoms (H₂O-Cu₅) arranged at nearest neighbor sites in the first and second layers of the Cu(100) surface (see Fig. 6). We performed systematic optimizations with regard to the molecular internal coordinates in addition to its location and orientation with respect to the metallic cluster. The binding energies of the complexes (relative to the separated H₂O and metal) in the calculated optimized configurations are 0.76 and 0.38 eV for H₂O-Cu and H₂O-Cu₅, respectively, in accord with experimental estimates of molecular H₂O adsorption energies on metals.^{19,21} Bonding occurs via coupling of the H₂O lone-pair orbitals to the metal states with an associated charge transfer to the metal of $\sim 0.15e$. As a consequence of the bonding mechanism, in the equilibrium geometry the oxygen end of the molecule points toward the metal cluster situated at a distance of 2.2 Å (2.0 Å for H₂O-Cu) with the H₂O molecular axis tilted with respect to the Cu-O bond by angles of 67° and 70° for the single Cu and Cu₅ clusters, respectively. (The molecular internal coordinates change only slightly upon adsorption.)

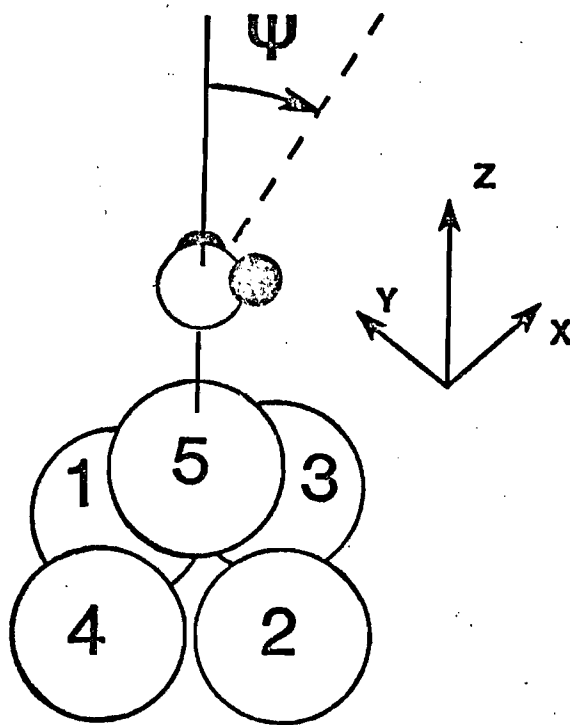


Fig. 6 Schematic picture of the H₂O-Cu₅ configuration. Numbered open circles denote Cu atoms. The oxygen atom is represented by an open circle and the hydrogens by solid circles. The molecular H₂O plane is tilted from the Cu(5)-O axis by the angle $\psi=70^\circ$.

In the equilibrium configuration of H_2O , the O-H bond length is 0.968 \AA [the experimental value (Ref. 22) is 0.957 \AA and the H-O-H angle is 105.3° [the experimental value (Ref. 22) is 104.52°] with a dipole moment of 2.02D [the experimental value (Ref. 22) is 1.88D]. The vibrational frequencies calculated from a 14-point fit to the potential surface in the vicinity of the equilibrium configuration including quadratic, cubic, and angle-bending bond-stretch cross terms are 228, 463, and 470 meV for the H-O-H bending, O-H symmetric and antisymmetric stretches, respectively, in close agreement with measured values²² (198, 453, 466 meV, respectively).

We turn now to a discussion of comparative studies of the interaction of H_2O with a single-Cu atom and a Cu_5 atomic cluster. The ground-state binding energies determined via systematic mappings of the potential-energy surfaces are $E_B(\text{H}_2\text{O}-\text{Cu}) = 0.76 \text{ eV}$ and $E_B(\text{H}_2\text{O}-\text{Cu}_5) = 0.38 \text{ eV}$. In the equilibrium geometry of the $\text{H}_2\text{O}-\text{Cu}$ system, bonding to the Cu is via the oxygen located at a distance $R_{\text{Cu}-\text{O}} = 2.0 \text{ \AA}$, with an O-H bond length $R_{\text{O}-\text{H}} = 0.98 \text{ \AA}$, a H-O-H angle $\gamma = 105^\circ$ and a Cu-O-H angle $\alpha = 103.6^\circ$ (i.e., the molecular H_2O plane is tilted by an angle $\psi = 67^\circ$ from the Cu-O axis). The corresponding values for the equilibrium $\text{H}_2\text{O}-\text{Cu}_5$ system are $R_{\text{Cu}-\text{O}} = 2.2 \text{ \AA}$, $R_{\text{O}-\text{H}} = 0.98 \text{ \AA}$, $\gamma = 106^\circ$, and $\alpha = 100.6^\circ$ ($\psi = 70^\circ$). Rotations about the Cu-O axis are essentially unhindered. Note that the H_2O structural parameters are close to those of the free molecule except for a slight increase of the O-H bond length which is consistent with the charge transfer, and that the structure is modified only slightly upon increasing the cluster size.

The nature of the bonding is best described using the orbital correlation diagrams (ocd) shown in Fig. 7 deduced from analysis of the orbital coefficients and the Mulliken population analysis shown in Table II. We emphasize that the Mulliken population analysis is employed as a guide in identifying orbital

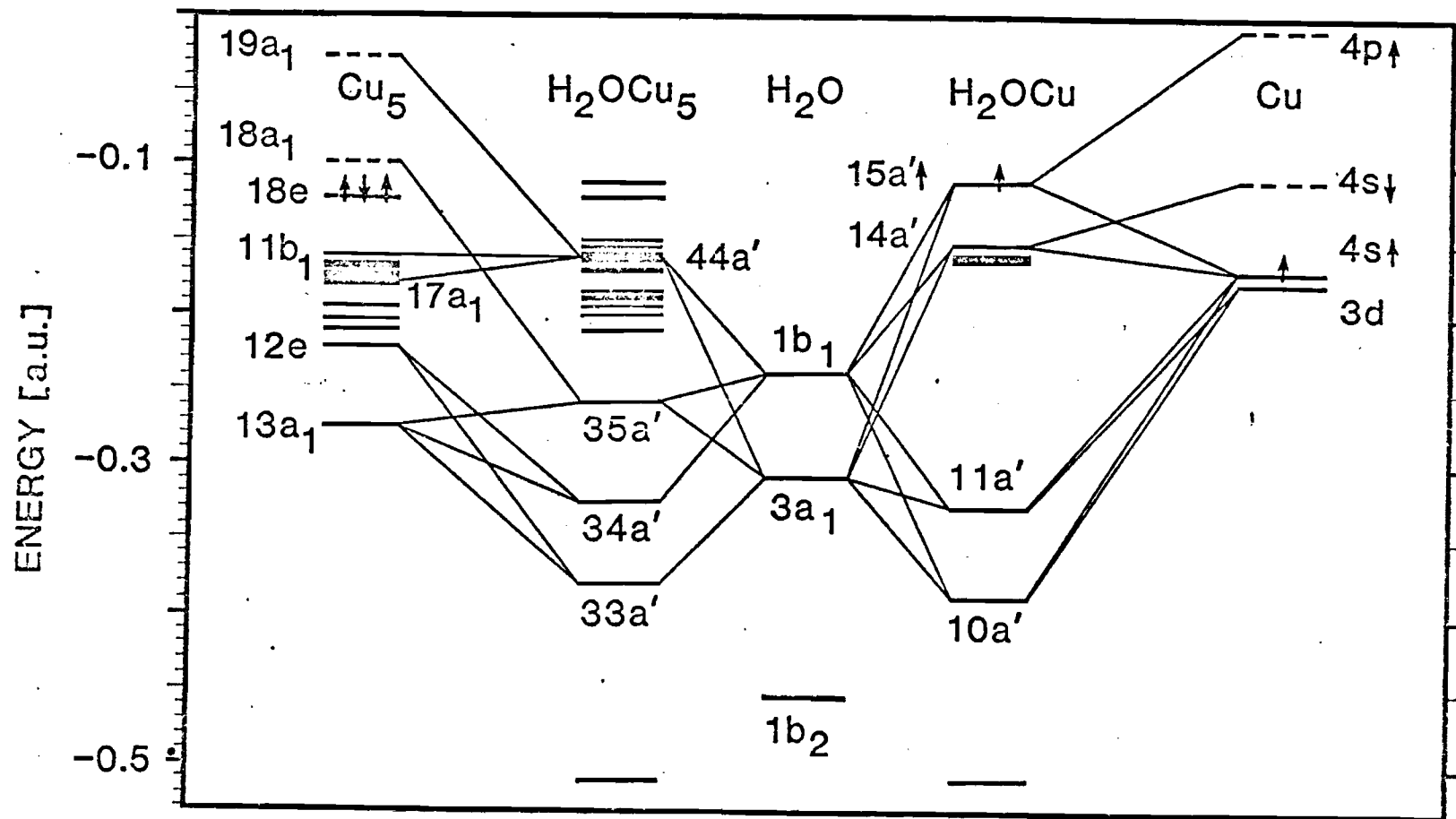


Fig. 7 Orbital-energy correlation diagrams for the equilibrium configurations of $\text{H}_2\text{O-Cu}$ and $\text{H}_2\text{O-Cu}_5$ obtained via spin-unrestricted SCF-LCAO with local X alpha exchange calculations. Occupied and partially occupied levels are denoted by solid lines; broken lines denote unoccupied levels.

Table II. Mulliken atomic populations for Cu atoms
in Cu_5 , $\text{H}_2\text{O-Cu}_5$, and $\text{H}_2\text{O-Cu}$.

	<i>s</i>	<i>p</i>		<i>d</i>	<i>f</i>	Total
$\text{H}_2\text{O-Cu}_5$						
Cu(1)	6.706	12.348		9.945	...	28.999
Cu(2)	6.706	12.348		9.945	...	28.999
Cu(3)	6.811	12.259		9.955	...	29.025
Cu(4)	6.873	12.237		9.933	...	29.043
Cu(5)	6.552	12.508		9.957	0.062	29.079
Total	33.648	61.70		49.735	0.062	145.145
$\text{H}_2\text{O-Cu}$						
Cu	7.122	12.107		9.904	0.017	29.15
Cu_5						
Cu(1-4)	6.748	12.291		9.931	...	28.97
Cu(5)	6.697	12.490		9.877	0.057	29.121
Total	33.689	61.654		49.601	0.057	145.00

admixture, and is used in conjunction with detailed analysis of orbital composition and electron-density distributions. Note also that while a small amount of charge transfer from the Cu d-atomic states is seen in the population analysis, the molecular orbitals of predominantly d character are fully occupied in all our calculations involving Cu, in agreement with experimental and theoretical findings.²³ Both our H₂O-metal clusters are of C_s symmetry leading to classification of the molecular orbitals according to their symmetry under reflection in the plane containing the Cu-O and the molecular H-O-H axes (A'-symmetric and A''-antisymmetric representations).

An explanation of the binding mechanisms of H₂O to Cu systems must invoke the participation of unoccupied and/or partially occupied orbitals, since combinations of the H₂O lone-pair orbitals (LPO's), 1b₁ (π-LPO) and 3a₁ (σ-LPO), with the metal fully occupied orbitals form bonding and antibonding orbitals with net zero bond order (the same argument was used in a recent study of H₂O binding to an Al cluster²⁴).

The equilibrium orientation of the bonded H₂O molecule reflects the energy dependence on the tilt angle ψ . Variations in this angle influence the amount of admixture between the H₂O LPO's and the metal orbitals (MO). In particular, the H₂O 3a₁-metal orbital admixture is large at $\psi = 0^\circ$ and, as $\psi \rightarrow \pi/2$, decreases as the H₂O 1b₁-metal orbital admixture increases.

In addition we have calculated the total dipole moment of the complex in terms of the electronic and nuclear-charge distributions. The charge donation to the metal is manifested via comparison of the dipole moment for the equilibrium configuration of H₂O-Cu₅ with those of Cu₅ and H₂O obtained by separating these components of the equilibrium complex to infinity:

$\mu(\text{H}_2\text{O}-\text{Cu}_5) = (1.2, 0.0, 3.2)$, $\mu(\text{H}_2\text{O}) = (2.0, 0.0, 0.65)$, $\mu(\text{Cu}_5) = (0.0, 0.0, 0.6)$
in Debye units. Associated with this value of $\mu(\text{H}_2\text{O}-\text{Cu}_5)$ is a work function

change $\Delta\phi \approx -4.8$ eV, for a surface density of 10^{15} molecules per square centimeter. The only available experimental values¹⁹ are for hydrogen-bonded water clusters and are typically $\Delta\phi \approx -1$ eV, indicating strong cancellation and depolarization effects.

It is of interest to note that the mechanism of H_2O binding to Cu clusters which we described is similar to that proposed recently for H_2O binding to a simple metal (Al) cluster.²⁴ Moreover, the equilibrium configuration and magnitudes of the binding energy and charge transfer are found to be similar for these two systems, suggesting common trends in the weak associative binding of molecular H_2O to metals. Finally, while convergence to the semi-infinite metal case may require clusters larger than those used by us, comparison of our results for H_2O -Cu and H_2O -Cu₅ and the agreement with experimental observations lead us to conclude that calculations employing small clusters can allow elucidation of binding mechanisms and provide quantitative estimates of physical properties in weakly bonded adsorption systems.

VI. References

1. S. Prakash and S. K. Joshi, Phys. Rev. B 2, 915 (1970).
2. W. Hanke, Phys. Rev. B 8, 4591 (1973).
3. M. W. Ribarsky, High Pressure in Science and Technology (Elsevier, New York, 1984).
4. W. Hanke and L. J. Sham, Phys. Rev. B 12, 4501 (1975).
5. M. W. Ribarsky, to be submitted.
6. Y. Takada, J. Phys. Soc. Jpn. 45, 786 (1978).
7. N. B. Brandt, S. V. Kuvshinnikov, A. O. Rusakov and V. M. Smernov, JETP Lett. 27, 33 (1978).
8. C. W. Chu, A. P. Rusakov, S. Huang, S. Early, T. H. Geballe and C. Y. Huang, Phys. Rev. B 18, 2116 (1978).
9. I. Leffowitz, J. S. Manning and P. E. Bloomfield, Phys. Rev. B 20, 4506 (1979).
10. A. B. Kunz and R. S. Weidman, J. Phys. C 12, L371 (1979).
11. A. Zunger and M. L. Cohen, Phys. Rev. B 20, 1189 (1979).
12. L. Kleinman and K. Mednick, Phys. Rev. B 20, 2487 (1979).
13. T. C. Collins, M. Seel and J. J. Ladik, Phys. Rev. B 27, 140 (1983).
14. M. Cardona, Phys. Rev. 129, 69 (1963).
15. J. C. Slater, Symmetry and Energy Bands in Crystals (Dover, New York, 1972). p. 347.
16. A. J. H. Wachters, J. Chem. Phys. 52, 1033 (1970).
17. E. Fiorino and R. Del Sole, Phys. Stat. Sol. B 119, 315 (1983).
18. M. W. Ribarsky, W. Luedtke and Uzi Landman, 44th Physical Electronics Conf. (June, 1984).
19. S. Andersson, C. Nyberg and C. G. Tengstal, Chem. Phys. Lett. 104, 305 (1984).
20. M. W. Ribarsky, W. Luedtke, and Uzi Landman, Phys. Rev. B 32, 1430 (1985).
21. K. Bange, D. E. Grider, J. K. Sass, and T. E. Madey, Surf. Sci. 136, 38 (1984).

22. W. S. Benedict, N. Gailar, and E. K. Plyler, J. Chem. Phys. 24, 1139 (1956).
23. J. R. Smith, J. G. Gay, and F. J. Arlinghaus, Phys. Rev. B 21, 2201 (1980).
24. J. E. Muller and J. Harris, Phys. Rev. Lett. 53, 2443 (1984).